IEEE Access
Multidisciplinary | Rapid Review | Open Access Journal

Received 7 May 2023, accepted 18 May 2023, date of publication 31 May 2023, date of current version 9 June 2023.

Digital Object Identifier 10.1109/ACCESS.2023.3281556

RESEARCH ARTICLE

Iterative Contraction Stability Control Strategy for Planar Prismatic-Rotational Underactuated Robot

ZIXIN HUANG[1,2,3], (Member, IEEE), **SHAOQI WEI**[1], **ZHEN CHEN**[2], AND **LEJUN WANG**[4]

[1]School of Electrical and Information Engineering, Wuhan Institute of Technology, Wuhan 430205, China
[2]Hubei Key Laboratory of Digital Textile Equipment, Wuhan Textile University, Wuhan 430200, China
[3]Hubei Key Laboratory of Intelligent Robot, Wuhan Institute of Technology, Wuhan 430205, China
[4]Chongqing Key Laboratory of Complex Systems and Bionic Control, Chongqing University of Posts and Telecommunications, Chongqing 400065, China

Corresponding author: Lejun Wang (wanglj@cqupt.edu.cn)

This work was supported in part by the Science and Technology Research Project of Hubei Provincial Education Department under Grant D20211506; in part by the Scientific Research Foundation of the Wuhan Institute of Technology under Grant K2021027; in part by the Hubei Key Laboratory of Intelligent Robot, Wuhan Institute of Technology, under Grant HBIRL202105; in part by the Hubei Key Laboratory of Digital Textile Equipment, Wuhan Textile University, under Grant KDTL2022003; and in part by the Graduate Innovative Fund of Wuhan Institute of Technology under Grant CX2022123 and Grant CX2022149.

ABSTRACT An iterative contraction stability control strategy is proposed to solve the end point position control problem of the planar prismatic-rotational (PR) underactuated robot. We establish the dynamic model of the planar PR underactuated robot, and use the algebra method to derive the nilpotent approximation model (NAM) with similar characteristics to the original system. According to the robot structure and control objectives, we propose a two-stage control idea: 1) Design a sliding mode variable structure controller to ensure that the active link can back to the target position after subsequent iterative operations; 2) Design an open-loop iterative control strategy based on the previous NAM to control the active link for iterative operation. The underactuated link is indirectly controlled and stabilized at any different accessible position under the action of the coupling relationship between links by controlling the active link. Finally, the simulation results prove that the end point of the robot can be effectively controlled to any positions.

INDEX TERMS Planar prismatic-rotational underactuated robot, nonholonomic system, iterative control, nilpotent approximation.

I. INTRODUCTION

The underactuated robot with fewer independent inputs than degrees of freedom is an important research object in the field of nonlinear control. It has the advantages of energy saving, light weight and flexibility [1], [2], which has brought a research boom in recent decades [3]. Aircraft [4], surface vessel [5] and bionic robot [6] are typical underactuated robot working in specific environments. The underactuated robot is formed for the following reasons: (1) Partial actuators of the full-actuated robot are damaged [7]; (2) Removing partial actuators to reduce cost, energy consumption and weight [8]; (3) The robot has natural underactuated characteristic. Therefore, the research on underactuated robot in various scenarios not only enriches the control strategy, but also promotes the development of nonlinear control theory [9], [10].

The associate editor coordinating the review of this manuscript and approving it for publication was Yangmin Li.

The planar underactuated robot is a typical research object suitable for the microgravity environment like space and deep sea. Any accessible points of such robot are equilibrium points, but the linear approximate model of the robot is uncontrollable at these points, which increases the difficulty of control [11], [12], [13]. The planar two-link underactuated robot is the foundation of the research on the planar underactuated robot [14], [15], [16], [17], [18], [19]. Ref. [20] established an accurate model of the planar rotational-prismatic (RP) underactuated robot by using the Gibbs-Appel formula in recursive form. Ref. [21] proved that planar PR underactuated robot had strong instability and motion irregularity by analyzing its motion equation. Ref. [22] constructed a control equation that only retained the angular velocity and acceleration of the passive joint, and designed a combined controller with the brake to realize point-to-point control of the planar PR underactuated robot. Although the use of combined controllers improved the control accuracy, it greatly increased the difficulty of design. In order to simplify the design difficulty, Ref. [23] designed the quintic interpolating spline auxiliary input for the controller to make the planar PR underactuated robot exponentially converge to the desired equilibrium configuration. The designed quintic interpolating spline auxiliary input could effectively shorten the stability control time, but it required a lot of calculation to solve unknown parameters, and the uncertainty of symbol attribute also brought difficulties to the design.

The planar underactuated robot was usually designed with multiple links to meet the needs of complex tasks [24], [25], [26]. Ref. [27] proposed a unified motion planning and intelligent optimization method for the planar four-link underactuated robot, which realized the stability control objective of the underactuated link at any positions. Ref. [28] analyzed the passivity of the planar prismatic-prismatic-rotational (PPR) robot, and designed the controller based on the energy method to realize the control objective, but the whole control time was long. Ref. [29] transformed the kinematic equation of the planar PPR robot into a chained form, and constructed the discontinuous feedback controller to realize the point-to-point control objective. This method greatly shorten the control time. Ref. [30] used a Lyapunov direct method and backstepping technique to construct a time-varying feedback controller, which made the planar PPR underactuated robot asymptotically converge to the desired states.

The control methods of the above planar multi-link underactuated robot are usually based on the exploration and promotion of the planar two-link underactuated robot. Therefore, this paper proposes an iterative contraction stability control strategy for a planar PR underactuated robot to solve the end point position control problem. Firstly, the dynamic model is built and the NAM with the same characteristics as the original system is obtained. According to the model structure and control objective of the planar PR underactuated robot, a two-stage control idea is presented: (1) Design the controller to realize the position control objective of the active link; (2) Design an open-loop iterative control strategy based on the NAM to make the underactuated link contract to the desired states. At last, the feasibility of the proposed control strategy for planar PR underactuated robot is proved.

The main contributions of this work are listed as follows:

- The proposed period control input with trigonometric function has the advantages of fewer parameters, fewer computation and its own symbolic attributes and so on.
- The proposed strategy can be applied to the other planar robot with a last underactuated link.

II. MODEL

This section describes the dynamic model of the planar PR underactuated robot and obtains the NAM with similar characteristics to the original system.

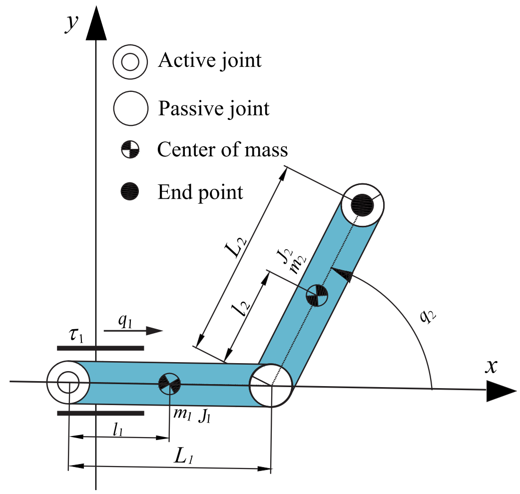

FIGURE 1. Model of the planar PR underactuated robot.

A. DYNAMIC MODEL

Figure 1 shows the model of the planar PR underactuated robot. The first active link moves laterally under the action of control torque $\boldsymbol{\tau} = [\tau_1, 0]^T$, and the second underactuated link rotates freely. τ_1 denotes the control torque applied to the active joint. The structure parameters of the r-th($r = 1, 2$) link: L_r is length, l_r is the distance from its joint to center of mass, q_r is angle, m_r is mass, and J_r is the moment of inertia.

The dynamic model is as follow

$$\boldsymbol{M}(\boldsymbol{q})\ddot{\boldsymbol{q}} + \boldsymbol{H}(\boldsymbol{q}, \dot{\boldsymbol{q}}) = \boldsymbol{\tau} \tag{1}$$

where the vector $[\boldsymbol{q}, \dot{\boldsymbol{q}}, \ddot{\boldsymbol{q}}]^T = [q_1, q_2, \dot{q}_1, \dot{q}_2, \ddot{q}_1, \ddot{q}_2]^T$ contains the angles, angular velocities and angular accelerations. $\boldsymbol{M}(\boldsymbol{q})$ is the inertia matrix with the characteristic of the symmetric positive definite, and $\boldsymbol{H}(\boldsymbol{q}, \dot{\boldsymbol{q}})$ contains the Coriolis and centrifugal forces,

$$\boldsymbol{M}(\boldsymbol{q}) = \begin{bmatrix} m_1 + m_2 & -m_2 l_2 \sin q_2 \\ -m_2 l_2 \sin q_2 & m_2 l_2^2 + J_2 \end{bmatrix}$$
$$\boldsymbol{H}(\boldsymbol{q}, \dot{\boldsymbol{q}}) = \begin{bmatrix} -m_2 l_2 \dot{q}_2^2 \cos q_2 \\ 0 \end{bmatrix} \tag{2}$$

Let $x = [x_1, x_2, x_3, x_4]^T = [q_1, q_2, \dot{q}_1, \dot{q}_2]^T$, the state space equation can be rewritten as

$$\dot{x} = f(x) + g(x)\tau \Leftrightarrow \begin{bmatrix} \dot{x}_1 \\ \dot{x}_2 \\ \dot{x}_3 \\ \dot{x}_4 \end{bmatrix} = \begin{bmatrix} x_3 \\ x_4 \\ f_1 \\ f_2 \end{bmatrix} + \begin{bmatrix} 0 & 0 \\ 0 & 0 \\ g_{11} & g_{12} \\ g_{21} & g_{22} \end{bmatrix} \begin{bmatrix} \tau_1 \\ 0 \end{bmatrix} \tag{3}$$

where

$$\begin{cases} [f_1, f_2]^T = -\boldsymbol{M}^{-1}(\boldsymbol{q})\boldsymbol{H}(\boldsymbol{q}, \dot{\boldsymbol{q}}) \\ \begin{bmatrix} g_{11} & g_{12} \\ g_{21} & g_{22} \end{bmatrix} = \boldsymbol{M}^{-1}(\boldsymbol{q}) \begin{bmatrix} 1 & 0 \\ 0 & 0 \end{bmatrix} \end{cases} \tag{4}$$

B. NILPOTENT APPROXIMATION MODEL

The underactuated portion in (1) is

$$(-m_2 l_2 \sin q_2)\ddot{q}_1 + (m_2 l_2^2 + J_2)\ddot{q}_2 = 0 \tag{5}$$

Let $A = \ddot{q}_1$, so

$$\ddot{q}_2 = \frac{m_2 l_2}{m_2 l_2^2 + J_2} \sin q_2 A \tag{6}$$

Combining with (1), (2), (5) and (6), we get

$$\tau_1 = \left(m_1 + m_2 - \frac{m_2^2 l_2^2}{m_2 l_2^2 + J_2} \sin^2 q_2 \right) A - m_2 l_2 \dot{q}_2^2 \cos q_2 \tag{7}$$

Let $C = m_2 l_2 / (m_2 l_2^2 + J_2)$. Combining with (6), we can get a new state space equation:

$$\dot{x} = h(x) + k(x)A \tag{8}$$

where A can be regard as a new control input, and

$$\begin{cases} h(x) = [\dot{q}_1, \dot{q}_2, 0, 0]^T \\ k(x) = [0, 0, 1, C \sin q_2]^T \end{cases} \tag{9}$$

Equation (8) is still subjected to the second-order nonholonomic constraint, which makes the constraint relationship of the robot unable to be integrated. Therefore, we construct accessibility matrix K_0 at initial states $x_0 = [q_1^0, q_2^0, \dot{q}_1^0, \dot{q}_2^0]^T$ based on (8) and compute the Lie brackets of vector fields h and k:

$$K_0 = [h \;\; k \;\; [h, k] \;\; [k, [h, k]]]_{x = x_0} \tag{10}$$

where the numbers of time that each vector field inside K_0 needs to perform the Lie bracket operation is: [0 0 1 2]. Then, we use $y = K_0^{-1}(x - x_0)$ to compute the Local coordinate at x_0, and construct the privileged coordinates [31]:

$$z_i = y_i + \sum_{v=2}^{w_i - 1} o_v(y_1, \ldots, y_{i-1}), \quad (i = 1, 2, 3, 4) \tag{11}$$

where $w_i = [1\ 1\ 2\ 3]$ is the numbers of time that each vector field in (10) perform the Lie bracket operation plus 1, and

$$o_v = -\sum_{\substack{\sum_{j=1}^{n} \alpha_j = v \\ \sum_{j=1}^{n} w_j \alpha_j < w_i}} \prod_{j=1}^{i-1} \left(\frac{y_j^{\alpha_j}}{\alpha_j}\right) \gamma_1^{\alpha_1} \ldots \gamma_{i-1}^{\alpha_{i-1}} \left(y_i + \sum_{e=2}^{v-1} o_e\right)(x_0) \tag{12}$$

The obtained privileged coordinates $z = [z_1, z_2, z_3, z_4]^T$ retains the accessibility of the original system. By using Taylor expansion to process the privileged coordinates, we obtain the NAM as

$$\dot{z} = \begin{bmatrix} 1 \\ 0 \\ -z_2 \\ 0 \end{bmatrix} + \begin{bmatrix} 0 \\ 1 \\ 0 \\ -\dfrac{(\dot{q}_2^I z_1)^2}{4C \cos q_2^I} - \dfrac{1}{2} z_3 \end{bmatrix} A \tag{13}$$

where q_2^I and $\dot{q}_2^I$ denote the angle and angular velocity of the underactuated link at the beginning of each cycle, respectively. Equation (13) and Equation (8) have exactly the same characteristics. Therefore, the subsequent control strategy can be designed based on Equation (13).

III. CONTROL METHOD DESIGN

A. CONTROL IDEA

Based on the model structure and control objective, a two-stage control idea is planned for the robot.

Stage 1: A sliding mode variable structure controller is designed for the active link to realize the target position, and to drive the free rotating underactuated link to satisfy the iterative initial conditions.

Stage 2: An open-loop contraction iterative control strategy is designed for the planar PR underactuated robot based on the NAM, so the states of underactuated link converge to the desired values under the action of the iterative control input.

B. CONTROLLER DESIGN OF STAGE 1

According to (3), the sliding mode surface is constructed as

$$S = \mu q_1(t) + \dot{q}_1(t) \tag{14}$$

Its derivative is

$$\dot{S} = \mu \dot{q}_1(t) + f_1 + g_{11}\tau_1 \tag{15}$$

Let

$$\dot{S} = \phi S - \varepsilon sgn(S) \tag{16}$$

where $sgn(S)$ denotes the sign of S, and μ, ϕ, ε are greater than zero.

The controller is designed as

$$\tau_1 = (-\phi S - \varepsilon sgn(S) - \mu \dot{q}_1(t) - f_1)\, g_{11}^{-1} \tag{17}$$

The Lyapunov function is constructed as

$$V = \frac{1}{2}(S)^2 \tag{18}$$

and its derivative is

$$\dot{V} = S\dot{S} = -\phi S^2 - \varepsilon |S| \leq 0 \tag{19}$$

According to the LaSalle's theorem [32], when $\dot{V} \equiv 0$, $S \equiv 0$, that is, $q_1(t) \to q_1^d$ and $\dot{q}_1(t) \to 0$. q_1^d denotes the target angle of the active link. Thus, the objective of ***Stage* 1** is realized, but the underactuated link may not have reached the target states, so we design an open-loop iterative control strategy to stabilize the underactuated link in ***Stage* 2**.

C. CONTROL DESIGN OF STAGE 2

Based on (13), we set $t = 0$ as the start time and the first link can back to target states with zero velocity. The control input $A(t)$ must meet

$$\int_0^T A(t)dt = 0, \int_0^T \int_0^t A(b)dbdt = 0 \tag{20}$$

According to (13) and (20), $z_2(T) = z_3(T) = 0$, we obtain the following errors relations

$$\begin{cases} \Delta q_2 = q_2^{II} - q_2^{I} = \dot{q}_2^{I} z_1(T) = \dot{q}_2^{I} T \\ \Delta \dot{q}_2 = \dot{q}_2^{II} - \dot{q}_2^{I} = C^2 \sin 2q_2^{I} \end{cases} \tag{21}$$

where q_2^{II} and $\dot{q}_2^{II}$ denote the angle and angular velocity of the underactuated link at the end of each cycle, respectively. q_2^d denotes the target angle of the underactuated link.

By calculating (20) and (13), we obtain

$$\Delta \dot{q}_2 = -C^2 \sin q_2^I \cos q_2^I \int_0^T z_2^2(t)dt + C(\dot{q}_2^I)^2 \sin q_2^I \int_0^T z_3(t)dt \tag{22}$$

Based on the above analysis, the following period control input is designed

$$A(t) = \begin{cases} -B\cos\dfrac{4\pi t}{T}, & t \in \left[0, \dfrac{T}{2}\right) \\ B\cos\dfrac{4\pi\left(t-\frac{T}{2}\right)}{T}, & t \in \left[\dfrac{T}{2}, T\right] \end{cases} \tag{23}$$

where B is the maximum absolute value of each cycle, the period control input is shown in FIGURE 2.

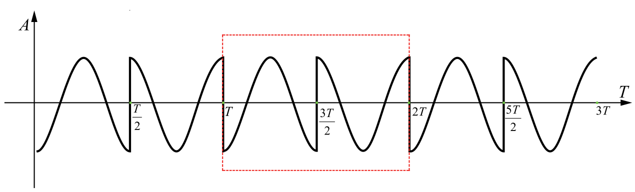

FIGURE 2. The period control input.

Remark: Compared with the quintic interpolating spline input in traditional method, the period control input with trigonometric function in this paper has the advantages of fewer parameters, fewer computation and its own symbolic attributes and so on.

According to (20) to (23), we obtain

$$\Delta \dot{q}_2 = -\frac{B^2 T^3 C^2}{64\pi^2} \sin 2q_2^I \tag{24}$$

The following relationships are set to ensure that the underactuated link contracts iteratively in each cycle

$$\left|q_2^d - q_2^{II}\right| \le \eta_1 \left|q_2^d - q_2^I\right|, \quad \left|\dot{q}_2^{II}\right| \le \eta_2 \left|\dot{q}_2^I\right| \tag{25}$$

where $[\eta_1, \eta_2] \in [0, 1)$ are coefficients of convergence.

By calculating (21), (24) and (25), we obtain

$$T = (1-\eta_1)\frac{q_2^d - q_2^I}{\dot{q}_2^I}, \quad B = \frac{8\pi}{CT}\sqrt{\frac{(1-\eta_2)\dot{q}_2^I}{T\sin 2q_2^I}} \tag{26}$$

Such B and T must meet the conditions: $0 < T, B < \infty$. The states of the planar PR underactuated robot can converge

TABLE 1. Model parameters.

Link r	m_r(kg)	L_r(m)	l_r(m)	J_r(kg·m^2)
1	1.000	1.000	0.500	0.000
2	1.000	1.000	0.500	1.000

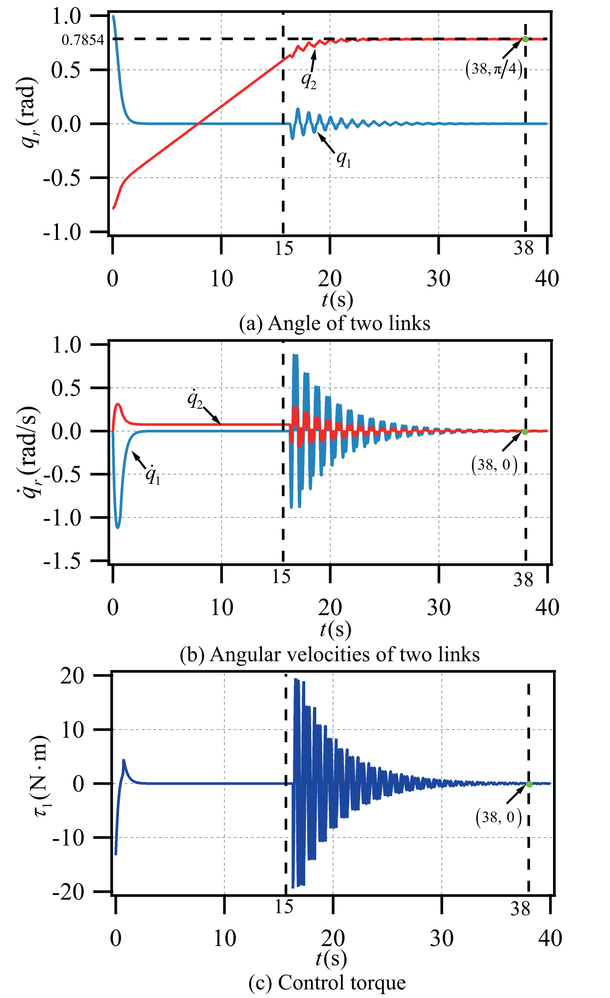

FIGURE 3. Simulation results of Case A.

when the following conditions are met:

$$\begin{cases} \dot{q}_2^I > 0 \\ q_2^d > q_2^I \\ q_2^I \in I \;\; or \;\; III \end{cases} \quad or \quad \begin{cases} \dot{q}_2^I < 0 \\ q_2^d < q_2^I \\ q_2^I \in II \;\; or \;\; IV \end{cases} \tag{27}$$

where I, II, III and IV represent that the rotation angle of the underactuated link is located at $(0 \pm 2k\pi, (\pi/2) \pm 2k\pi)$, $((\pi/2) \pm 2k\pi, \pi \pm 2k\pi)$, $(\pi \pm 2k\pi, (3\pi/2) \pm 2k\pi)$ and $((3\pi/2) \pm 2k\pi, 2\pi \pm 2k\pi)$, $(k = 1, 2, \ldots, n)$, respectively. The controller (7) of ***Stage* 2** controls the active link to perform iterative operation when the states of the underactuated link at the end of the ***Stage* 1** meet the one of the above set.

The designed auxiliary control input $A(t)$ is applied to the above controller (7). From the beginning of iteration t_1 to the end of iteration t_d, there are i iteration cycles T, that is, $t_d = t_1 + iT, (i = 1, 2, \ldots, n)$. The initial states is the end states of the last iteration operation. The states of

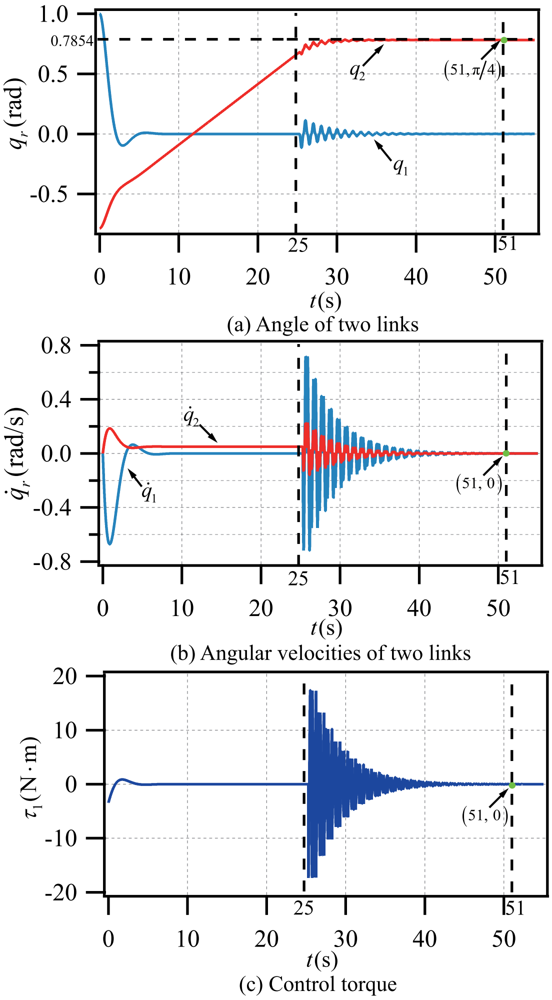

FIGURE 4. Simulation results of the PD controller.

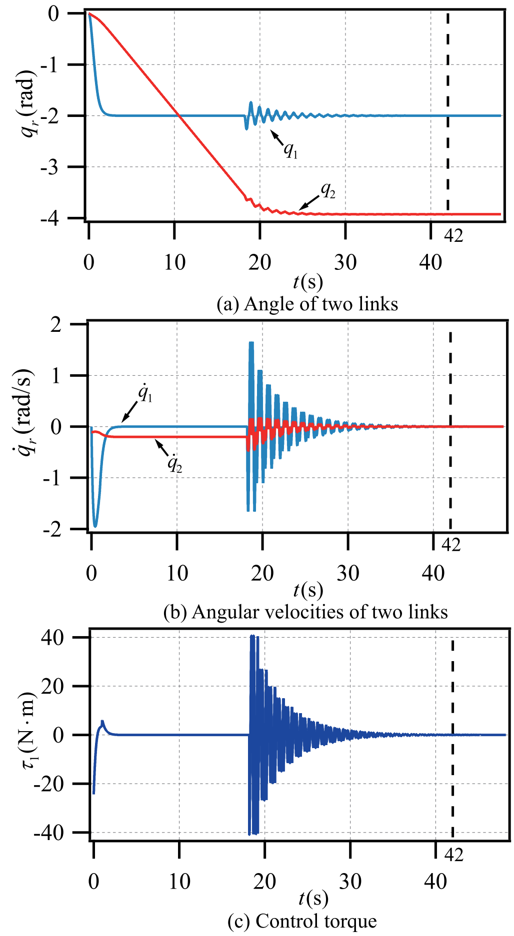

FIGURE 5. Simulation results of Case B.

underactuated link is close to the target stability states through repeated iterative contration operations. After n iteration, the planar PR underactuated robot is stabilized at the target states.

IV. SIMULATION

MATLAB/Simulink is used to simulate four cases where the end point of the planar PR underactuated robot is located in different positions. The parameters of the designed controller (17) and contraction rates are chosen as: $\mu = 2.6$, $\varepsilon = 2.0, \phi = 1.8, \eta_1 = \eta_2 = 0.6$. TABLE 1 shows the structure parameters.

A. CASE A

Considering the case that the rotation angle of the underactuated link is in $(0 \pm 2k\pi, (\pi/2) \pm 2k\pi)$, let the initial states as $x_0 = [1, -\pi/4, 0, 0]^T$ and the target states as $x_d = [0, \pi/4, 0, 0]^T$.

The simulation results (FIGURE 3(a) and FIGURE 3(b)) show that the states of the planar PR underactuated robot successfully converge to their target values at 38 s. The proposed strategy realizes the control objective of ***Stage* 1** at 15 s. FIGURE 3(c) shows that the control torque of the robot gradually approaches zero. The end point of the robot is quickly stabilized to the target position. Compared with the control method in Ref. [23], the end point of the robot converges to the target position at 48 s. Therefore, the proposed strategy in this paper can realize control objective faster.

Furthermore, we use the PD controller for simulation and comparison under the same conditions, where $P = 1.8$ and $D = 1.6$. FIGURE 4 shows that the active link reaches the target position at 25 s under the action of the PD controller. By comparing the control effects of two different controllers in ***Stage* 1**, the sliding mode variable structure controller controls the active link to the target position in shorter time.

B. CASE B

Considering the case that the rotation angle of the underactuated link is in $((\pi/2) \pm 2k\pi, \pi \pm 2k\pi)$, we set the initial and target states as $x_0 = [0, 0, 0, 0]^T$ and $x_d = [-2.0, -5\pi/4, 0, 0]^T$.

FIGURE 5 is the simulation results of Case B. The results show that when $t = 42$ s, the angle of each link reaches target value, the angular velocity of each link converges to zero, the control torque gradually decreases from about ± 43 N·m to 0 N·m. The end point of the robot is stabilized to the target position.

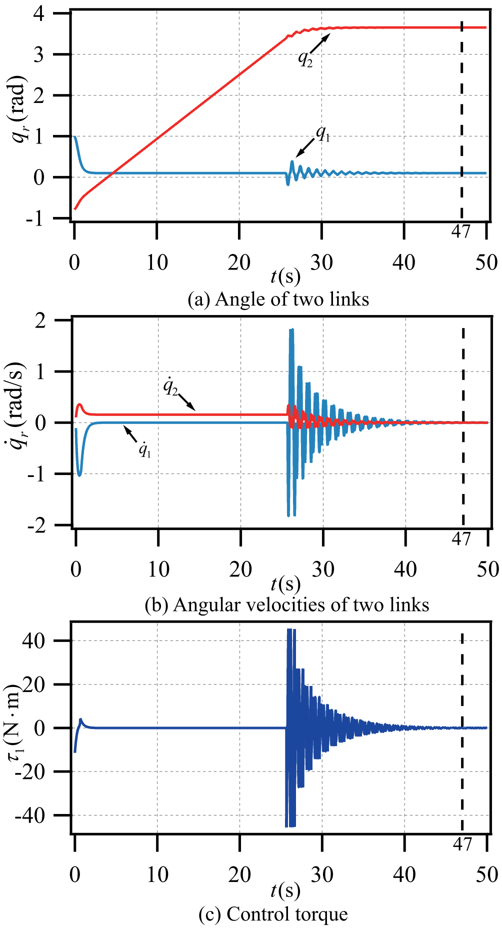

FIGURE 6. Simulation results of Case C.

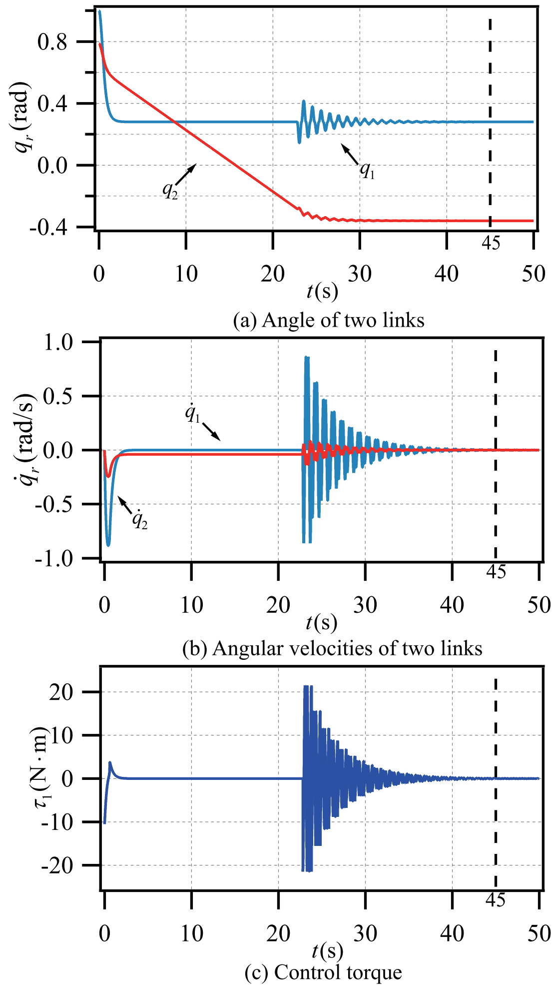

FIGURE 7. Simulation results of Case D.

C. CASE C

In order to verify that the proposed control strategy is also effective when the rotation angle of the underactuated link is in $(\pi \pm 2k\pi, (3\pi/2) \pm 2k\pi)$, we set the initial states as $x_0 = [1, -\pi/4, 0, 0]^T$ and the target states as $x_d = [0.1, 7\pi/6, 0, 0]^T$.

FIGURE 6(a) and FIGURE 6(b) show that the angles of two links gradually approach their objectives and the angular velocities converge to zero when $t = 47$ s. FIGURE 6(c) shows that the applied control torque to the active link gradually decreases from about ±50 N·m to 0 N·m in the subsequent cycles. The end point of the robot is successfully stabilized to the target position.

D. CASE D

Considering the case that the rotation angle of the underactuated link is in $((3\pi/2) \pm 2k\pi, 2\pi \pm 2k\pi)$, let the initial states as $x_0 = [1, \pi/4, 0, 0]^T$ and the target states as $x_d = [0.28, -4\pi/35, 0, 0]^T$.

FIGURE 7(a) and FIGURE 7(b) show that the states of the planar PR underactuated robot successfully converge to their target values within $t = 45$ s. FIGURE 7(c) shows that the required control torque for each cycle gradually decreases to 0 N·m in the contraction stage. The position control objectives of the end point are realized.

V. CONCLUSION

This paper presents an iterative contraction stability control strategy for a planar PR robot based on nilpotent approximation method. This strategy solves the end point position control problem of the robot. First, the dynamic model of the planar PR underactuated robot is established and the NAM with similar characteristics to the original system is obtained. Then, the sliding mode variable structure controller is used to realize the position control in ***Stage*** **1**; and the open-loop iterative control input is designed to realize the stability control of the robot in ***Stage*** **2**. Finally, the simulation results prove the feasibility of the iterative contraction stability control strategy for planar PR underactuated robot.

REFERENCES

[1] Z. Huang, X. Lai, P. Zhang, Y. Wang, and M. Wu, "Virtual model reduction-based control strategy of planar three-link underactuated manipulator with middle passive joint," *Int. J. Control, Autom. Syst.*, vol. 19, no. 1, pp. 29–39, Jan. 2021.

[2] T. Yang, N. Sun, and Y. Fang, "Neuroadaptive control for complicated underactuated systems with simultaneous output and velocity constraints exerted on both actuated and unactuated states," *IEEE Trans. Neural Netw. Learn. Syst.*, early access, Oct. 8, 2021, doi: 10.1109/TNNLS.2021.3115960.

[3] J. Huang, S. Ri, T. Fukuda, and Y. Wang, "A disturbance observer based sliding mode control for a class of underactuated robotic system with mismatched uncertainties," *IEEE Trans. Autom. Control*, vol. 64, no. 6, pp. 2480–2487, Jun. 2019.

[4] Y. Wang, "A novel sliding mode controller for underactuated vertical takeoff and landing aircraft," *Int. J. Circuits, Syst. Signal Process.*, vol. 14, pp. 34–41, Jan. 2020.

[5] B. S. Park and S. J. Yoo, "An error transformation approach for connectivity-preserving and collision-avoiding formation tracking of networked uncertain underactuated surface vessels," *IEEE Trans. Cybern.*, vol. 49, no. 8, pp. 2955–2966, Aug. 2019.

[6] Z. Huang, X. Li, J. Wang, Y. Zhang, and J. Mei, "Human pulse detection by a soft tactile actuator," *Sensors*, vol. 22, no. 13, pp. 5047–5056, 2022.

[7] M. Van and D. Ceglarek, "Robust fault tolerant control of robot manipulators with global fixed-time convergence," *J. Franklin Inst.*, vol. 358, no. 1, pp. 699–722, Jan. 2021.

[8] J. Li, L. Wang, Z. Chen, and Z. Huang, "Drift suppression control based on online intelligent optimization for planar underactuated manipulator with passive middle joint," *IEEE Access*, vol. 9, pp. 38611–38619, 2021.

[9] C. Pan, C. Cui, L. Zhou, P. Xiong, and Z. Li, "A model-free output feedback control approach for the stabilization of underactuated TORA system with input saturation," *Actuators*, vol. 11, no. 3, p. 97, Mar. 2022.

[10] N. Sun and Y. Fang, "Nonlinear tracking control of underactuated cranes with load transferring and lowering: Theory and experimentation," *Automatica*, vol. 50, no. 9, pp. 2350–2357, Sep. 2014.

[11] Z. Huang, S. Wei, M. Hou, and L. Wang, "Finite-time control strategy for swarm planar underactuated robots via motion planning and intelligent algorithm," *Meas. Control*, vol. 56, nos. 3–4, pp. 813–819, Mar. 2023, doi: 10.1177/00202940221116606.

[12] P. Zhang, X. Lai, Y. Wang, and M. Wu, "Chaos-PSO-based motion planning and accurate tracking for position-posture control of a planar underactuated manipulator with disturbance," *Int. J. Control, Autom. Syst.*, vol. 19, no. 10, pp. 3511–3521, Oct. 2021.

[13] M. R. J. Harandi, H. Damirchi, S. A. K. Seyedi, and H. D. Taghirad, "Point-to-point motion control of an underactuated planar cable driven robot," in *Proc. 27th Iranian Conf. Electr. Eng. (ICEE)*, Apr. 2019, pp. 979–984.

[14] X.-Z. Lai, J.-H. She, S. X. Yang, and M. Wu, "Comprehensive unified control strategy for underactuated two-link manipulators," *IEEE Trans. Syst., Man, Cybern., B Cybern.*, vol. 39, no. 2, pp. 389–398, Apr. 2009.

[15] Z. Huang, Y. Zhou, Z. Chen, W. Wang, and L. Wang, "An universal control strategy for planar 2-DoF underactuated manipulator with one passive joint," in *Proc. 40th Chin. Control Conf. (CCC)*, Jul. 2021, pp. 468–472.

[16] Z. Huang and X. Lai, "Control strategy based on iterative method for planar Pendubot," in *Proc. 37th Chin. Control Conf. (CCC)*, Jul. 2018, pp. 858–861.

[17] Y. Wang, X. Lai, and M. Wu, "Rapid position control approach based on variable design parameter for planar Acrobot," *Electr. Mach. Control*, vol. 21, no. 9, pp. 110–118, 2017.

[18] J. Wu, Y. Wang, W. Ye, and C.-Y. Su, "Control strategy based on Fourier transformation and intelligent optimization for planar Pendubot," *Inf. Sci.*, vol. 491, pp. 279–288, Jul. 2019.

[19] Z. Huang and L. Wang, "Review of control method of planar underactuated mechanical system," *J. Wuhan Inst. Technol.*, vol. 43, no. 4, pp. 448–454, 2021.

[20] M. H. Korayem and A. M. Shafei, "Motion equation of nonholonomic wheeled mobile robotic manipulator with revolute–prismatic joints using recursive Gibbs–Appell formulation," *Appl. Math. Model.*, vol. 39, nos. 5–6, pp. 1701–1716, Mar. 2015.

[21] S. Alaci, F. Ciornei, C. Suciu, and I. Romanu, "The effect of structural aspect for planar systems with 2DOF upon the stability of motion," in *Proc. IOP Conf. Mater. Sci. Eng.*, vol. 1169, May 2021, Art. no. 012003.

[22] L. Wu, X. Kuai, and G. Yang, "Nonholonomic control of a planar prismatic-revolute underactuated manipulator," in *Proc. Sci. Inf. Conf.*, Oct. 2013, pp. 144–147.

[23] A. De Luca, S. Iannitti, and G. Oriolo, "Stabilization of a PR planar underactuated robot," in *Proc. IEEE Int. Conf. Robot. Autom.*, May 2001, pp. 2090–2095.

[24] C. Urrea, J. Kern, and E. Álvarez, "Design of a generalized dynamic model and a trajectory control and position strategy for n-link underactuated revolute planar robots," *Control Eng. Pract.*, vol. 128, Nov. 2022, Art. no. 105316.

[25] X. Xin, "Linear strong structural controllability and observability of an n-link underactuated revolute planar robot with active intermediate joint or joints," *Automatica*, vol. 94, pp. 436–442, Aug. 2018.

[26] Z. Huang, X. Lai, P. Zhang, Q. Meng, and M. Wu, "A general control strategy for planar 3-DoF underactuated manipulators with one passive joint," *Inf. Sci.*, vol. 534, pp. 139–153, Sep. 2020.

[27] J. Wu, W. Ye, Y. Wang, and C. Su, "A general position control method for planar underactuated manipulators with second-order nonholonomic constraints," *IEEE Trans. Cybern.*, vol. 51, no. 9, pp. 4733–4742, Sep. 2021.

[28] I. Fantoni, "Stabilization of a planar prismatic-prismatic-revolute manipulator based on an energy approach," in *Proc. 40th IEEE Conf. Decis. Control*, Dec. 2001, pp. 3752–3757.

[29] A. D. Mahindrakar, R. N. Banavar, and M. Reyhanoglu, "Discontinuous feedback control of a 3 link planar PPR underactuated manipulator," in *Proc. 40th IEEE Conf. Decis. Control*, Dec. 2001, pp. 2424–2429.

[30] L.-C. Wu, G.-S. Yang, and Z.-Q. Sun, "A tracking control method for a PPR underactuated manipulator," in *Proc. ICCAS*, Oct. 2010, pp. 1255–1258.

[31] A. Isidori, *Nonlinear Control Systems*, 3rd ed. New York, NY, USA: Springer-Verlag, 1995.

[32] J. P. LaSalle, "Stability theory for ordinary differential equations," *J. Differ. Equ.*, vol. 4, no. 1, pp. 57–65, Jan. 1968.

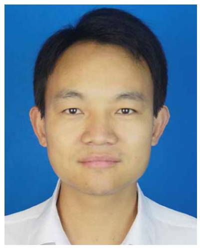

ZIXIN HUANG (Member, IEEE) received the B.S. and M.S. degrees in engineering from Wuhan Textile University, Wuhan, China, in 2013 and 2016, respectively, and the Ph.D. degree in engineering from the China University of Geosciences, Wuhan, in 2020. In 2020, he joined the Wuhan Institute of Technology, Wuhan, where he is currently a Lecturer with the School of Electrical and Information Engineering. His current research interests include robot control, nonlinear system control, and intelligent control. He is a Senior Member of the Chinese Association of Automation.

SHAOQI WEI is currently pursuing the M.S. degree in energy power engineering with the School of Electrical and Information Engineering, Wuhan Institute of Technology. His current research interests include robot control, nonlinear system control, and intelligent control.

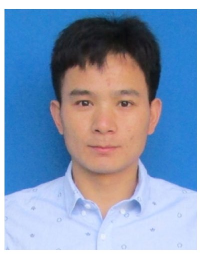

ZHEN CHEN received the B.S. and M.S. degrees in engineering from Wuhan Textile University, Wuhan, China, in 2011 and 2015, respectively. His current research interests include automation control and new textile machinery.

LEJUN WANG received the B.S. degree in electrical engineering and automation from Anyang Normal University, Anyang, China, in 2014, the M.S. degree in control science and engineering from Northeast Electric Power University, Jilin, China, in 2018, and the Ph.D. degree in engineering from the China University of Geosciences, Wuhan, China, in 2022. In 2022, he joined the Chongqing University of Posts and Telecommunications, Chongqing, China. His research interest includes the intelligent control technology of robot.